Shape Optimization of a Kind of Earth Embankment Type Windbreak Wall along the Lanzhou-Xinjiang Railway

J. Zhang[1, 2†], G. Gao[1, 2], T. Liu[1, 2] and Z. Li[1, 2]

[1] *Key Laboratory of Traffic Safety on Track of Ministry of Education, Changsha, Hunan 410075, China*
[2] *School of Traffic & Transportation Engineering, Central South University, Changsha, Hunan 410075, China*

†*Corresponding Author Email: jie_csu@csu.edu.cn*

ABSTRACT

In order to promote the windbreak effect of the earth embankment type windbreak wall, enhance the operational speed of the single passenger train and improve the quality of the pantograph-catenary current collection for a locomotive, a three-dimensional RANS turbulence model k-epsilon was used to optimize the shape of windbreak walls. The relationships between the overturning moment of trains, the lateral wind speed at the catenary position and the height (depth) in optimization projects were analyzed. Validation was performed against full-scale experimental data. To understand the flow field around the train with different types of windbreak walls, pressure contours and surface pressure coefficient distributions were investigated. The results show that for the original type windbreak wall, the overturning moment of the passenger car is a little larger. However, for the optimization projects, the trains are basically in a minor negative pressure environment and the aerodynamic forces are much less. The optimal heights of the heightening type (depths for the cutting type) do not change obviously as the train speed increases. When the passenger car stands on the track without movement, the optimal height/depth is the smallest. Behind the original type's windbreak wall, the lateral wind speed at the catenary position on the leeward line is less than that on the windward line. Meanwhile, as the train runs on the windward or leeward lines, the corresponding lateral wind speed rise sharply by 37.5% and 40.5%, respectively. After the adoption of optimized projects, the speeds of the two lines monotonically decrease. The best height of the heightening type is 0.30 m, and the optimal depth of the cutting type is 1.40 m. From the perspective of engineering application, the heightening type is a more suitable project.

Keywords: Railway; Windbreak wall; Optimization; Overturning moment; Catenary; Aerodynamics.

NOMENCLATURE

A	reference area	p	mean static pressure
C_l	lift force coefficient	p_{ref}	reference pressure
C_M	overturning moment coefficient	Re_c	critical Reynolds number
C_p	static pressure coefficient	Re	Reynolds number
C_s	side force coefficient	u_i	mean velocity vector
C_μ	turbulent constant	V_t	train speed
F_l	lift force	V_w	wind velocity
F_s	side force		
H	height of the heightening wall	ε	dissipation rate
h	height of the passenger car	μ	dynamic viscosity of air
k	turbulent kinetic energy	μ_t	eddy viscosity
L	depth of the cutting part	v	air kinematic viscosity
l	width of the passenger car	ρ	air density
M	overturning moment		

1. INTRODUCTION

Complex topography and Siberian cold waves along the Lanzhou-Xinjiang railway contribute 4 strong wind areas coming into being, named Baili Wind Region, Sanshili Wind Gap, Dabancheng Wind Gap and Alataw Pass Wind Gap. All these regions are administered by the Urumqi Railway Bureau (Ge *et al.* 2009), where the wind blows fiercely and frequently. On over 100 days per year, the wind level exceeds grade 8 (At grade 8, the wind velocity is in a range from 17.2m/s to 20.7 m/s) (Ge *et al.* 2009). The maximum instantaneous wind speed even reaches 60 m/s (Ge *et al.* 2009). More than 30 train-overturning accidents are estimated to have been caused by strong winds from 1960 to 2002 (Ge *et al.* 2009), and these incidents caused massive damage and economic loss. Thus, the gale disaster has become one of the major natural disasters along the Lanzhou-Xinjiang railway line.

Under strong winds, to improve train operational safety and railway transportation efficiency, a conventional approach is to build windbreak walls (Baker 1986 and 1999, Fauchier *et al.* 1999, Fujii *et al.* 1999, Bocciolone *et al.* 2008, Tomasini *et al.* 2015, Wang *et al.* 1990, Liu 2006, Zhang and Liu 2012 and 2014). In Europe and Japan, the windbreak walls that are made of perforated steel sheets are just straight with very thin thickness and uniform porosity. However, in Xinjiang of China, the wind condition is very complex and different. The trains run on the Lanzhou-Xinjiang railway line would be subjected to the desert wind, so the walls with porosity, except of these on the high bridges, will be not a good choice. To make full use of the local conditions and save the material resources, one common kind of windbreak walls along the Lanzhou-Xinjiang railway line is the earth embankment type that is formed by piling up gravel, as shown in Fig. 1. Some other types of walls are the reinforcement type, the concrete tie with plate type, the concrete type and the bridge type with holes. There are so many kinds of windbreak walls that Xinjiang has become an exhibition center.

Fig. 1. Earth embankment type windbreak wall along the Lanzhou-Xinjiang railway.

Generally, an obstacle may result in a shielding effect on the bodies behind it. The crosswind stability of trains behind a windbreak wall would be better than the train without walls. But if the train's top is higher than the height of the windbreak wall with an inclined windward side, the shielding effect will be not enough, and the flow still can act on the train body (Zhang and Liu 2012 and 2014). After that, as the train is running at a higher speed, it is still in a danger. To keep the safety of the train, the best way is to reduce the train speed. However, reducing the speed would cause lots of economic loss, which is not allowed by the Railway Bureaus. If the train is required to run at a normal or higher speed, it is urgently needed to improve the windbreak effect of the walls.

To assess the windbreak capacity of existing windbreak walls and provide references for their reconstruction, from March 2009 to June 2009, a comprehensive full-scale test of aerodynamic performance of trains and windbreak facilities along the Lanzhou-Xinjiang railway under strong winds were carried out by the Urumqi Railway Bureau who organized Central South University, China Academy of Railway Sciences, China Railway First Surver & Design Institute, China Railway Northwest Institute and Xinjiang Meteorology (Central South University 2011). The test was conducted 5 times, including the aerodynamics of 7 kinds of vehicles (2 kinds of passenger cars, 5 kinds of freight cars), vehicle dynamic offset, vehicle dynamics, aerodynamics of windbreak walls and vibration performance of the bridge type. According to the experimental data, all these indicate that there is a large difference in the windbreak effect between the earth embankment type and the other four types (Central South University 2011). The worst locations in terms of train aerodynamic characteristics and dynamic performances are the railway without windbreak walls, districts with the earth embankment type windbreak wall and the transition region between windbreak walls and cuts (Central South University 2011).

Concerning on above three cases, many publications mainly investigate the aerodynamic performance of trains under the condition without windbreak walls (Khier *et al.* 2000, Diedrichs *et al.* 2007, Cheli *et al.* 2010, Hemida and Krajnovic 2010, Baker 2010, Liu and Zhang 2013, Rezvani and Mohebbi 2014). However, research work at the conditions of the earth embankment type windbreak wall and the transition region between windbreak walls and cuts are relatively rare (Zhang and Liu 2012 and 2014, Wang 2010).

Zhang and Liu (2012) used the finite volume method to simulate the effect of the earth embankment type windbreak wall's slope angles on the aerodynamic force and moment coefficients of trains along the Xinjiang single-track railway line. Their simulations were based on the three-dimensional steady uncompressible N-S equation and k-ε turbulence model. And they discovered that the train aerodynamic coefficients were not sensitive to the leeward slope angle of walls, while their research objective was focused on the box wagon. Zhang and Liu (2014) also investigated the multistep design of the earth embankment type windbreak wall along the Lanzhou-Xinjiang

railway line. They found that this multistep design could improve the windbreak effect largely, but the lateral wind speed at the catenary position was not taken into consideration. Wang (2010) used a CFD method to analyze and optimize the aerodynamic performance of trains at a transitional zone between a cut and a windbreak wall, but the wall was not the earth embankment type. Based on these key points, in this paper, two new kinds of design projects are proposed to enhance the operational speed of the passenger train and improve the quality of the pantograph-catenary current collection for a locomotive behind the walls.

Single passenger trains are the main kind of passenger vehicles running on the Lanzhou-Xinjiang railway line. Thus, it is very important to guarantee the operational safety of such trains. The electrification construction of the Lanzhou-Xinjiang railway has been completed at the end of 2012, and the lateral wind speed at the catenary position has an obvious effect on the quality of the pantograph-catenary current collection for a locomotive. Thus, to promote the windbreak effect of the earth embankment type windbreak wall and improve the quality of the pantograph-catenary current collection of the locomotive, this paper first suggests an idea for optimization based on the straight windbreak wall. Then a comparison is made between the numerical and experimental results to validate the accuracy of the present numerical method. Aerodynamic loads of trains under strong winds are investigated to obtain the best sizes for two different projects. To discover the reason for the various aerodynamic loads, flow fields and surface pressure coefficients are analyzed. Finally, the lateral wind speed at the catenary position behind different windbreak walls is studied to complement the operational safety of trains in wind environments.

2. NUMERICAL METHOD

The resultant speed, which consists of the single passenger train speed and crosswind velocity, is no more than 100 m/s in the wind regions of Xinjiang, so the Mach number is less than 0.3 and the air around the train can be considered to be incompressible (Tian 2007). According to the work conducted by Zhang and Liu (2014), when the wind speed is more than 42 m/s, the train running on the railway line with a windbreak wall does not allow to pass through the wind region. Then based on the Beaufort scale, choose the least wind speed V_w = 41.4 m/s, and the wind direction is set as 90°. The width l of the passenger train is 3.105 m. The height above sea level of the Lanzhou-Xinjiang railway line in the Baili Wind Region varies from 500 m to 700 m. According to 'The Load Code for the Design of Building Structure (GB5009-2012)', the air density ρ should be 1.177kg/m^3. Subsequently, at the ambient temperature of 20°C, the air kinematic viscosity v = 1.54×10^{-5} m^2/s, and the Reynolds number $Re = V_w l/v$ =8.35×10^6 >> Re_c. Re_c is the critical Reynolds number for the laminar and turbulent flow. Taking the flow case into account, the Reynolds-averaged Navier-Stokes equations

(RANS) combined with the eddy viscosity hypothesis (Tian 2007, Fluent Inc. 2006) represent the most extensive method in engineering applications (Khier *et al.* 2000, Asgharzadeh *et al.* 2012, Zhang and Liu 2012 and 2014, Munoz-Paniagua *et al.* 2015) for computing the flow field.

In general, the equations are reduced to the following form (Fluent Inc. 2006).

Continuity:

$$\partial u_i / \partial x_i = 0 \tag{1}$$

Momentum:

$$\frac{\partial(\rho u_i u_j)}{\partial x_j} = -\frac{\partial p}{\partial x_i} + \frac{\partial}{\partial x_j}\left((\mu + \mu_t)\frac{\partial u_i}{\partial x_j}\right) \tag{2}$$

Where, u_i is the mean velocity vector. ρ is the air density with a constant. p is the mean static pressure. μ is the dynamic viscosity of air. The eddy viscosity μ_t is related to turbulent kinetic energy k and its rate of dissipation ε by the following relation when the k-ε model is used to close the above set of equations:

$$\mu_t = \rho C_\mu k^2 / \varepsilon \tag{3}$$

Where C_μ is a turbulent constant, k and ε are obtained from the standard k-ε turbulence model equations that can be expressed as follows:

Turbulence kinetic energy k:

$$\frac{\partial(\rho k u_i)}{\partial x_i} = \frac{\partial}{\partial x_j}\left[\left(\mu + \frac{\mu_t}{\sigma_k}\right)\frac{\partial k}{\partial x_j}\right]$$

$$+ \mu_t\left(\frac{\partial u_i}{\partial x_j} + \frac{\partial u_j}{\partial x_i}\right)\frac{\partial u_i}{\partial x_j} - \rho\varepsilon \tag{4}$$

Dissipation rate ε:

$$\frac{\partial(\rho \varepsilon u_i)}{\partial x_i} = \frac{\partial}{\partial x_j}\left[\left(\mu + \frac{\mu_t}{\sigma_\varepsilon}\right)\frac{\partial \varepsilon}{\partial x_j}\right]$$

$$+ C_{1\varepsilon}\frac{\varepsilon}{k}\mu_t\left(\frac{\partial u_i}{\partial x_j} + \frac{\partial u_j}{\partial x_i}\right)\frac{\partial u_i}{\partial x_j} - C_{2\varepsilon}\rho\frac{\varepsilon^2}{k} \tag{5}$$

Constant coefficients:

C_μ=0.09，$C_{1\varepsilon}$=1.44，$C_{2\varepsilon}$=1.92，σ_k=1.0，σ_ε=1.3 (6)

In this paper, the commercial CFD software Fluent was used, and the Finite Volume Method (FVM) based on cell centers was adopted for the discretization of the controlling equations. Simulations were performed using a pressure-based solver. A second-order upwind scheme was chosen to solve the momentum, k and ε equations. The SIMPLEC (Semi-Implicit Method for Pressure-Linked Equations-Consistent) algorithm was used in the computational method to couple the pressure and the velocity field. The convergence criterion was based on the residual value of the continuity equation being set at 10^{-6} with minimal fluctuation.
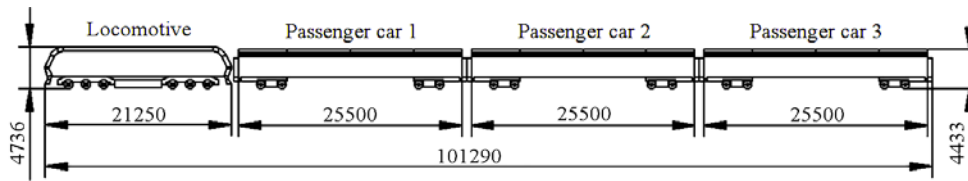
Fig. 2. Single passenger train (unit: mm).

Convergence was also monitored by plotting the aerodynamic force coefficients on the second passenger car until the variation of force became steady with iterations.

3. COMPUTATIONAL DETAILS

In the current paper, a simplified single passenger train was chosen as the research objective to improve the windbreak performance of the original earth embankment type windbreak wall. The train geometry is shown in Fig. 2. It consists of four cars with bogies and inter-carriage gaps, without the pantograph and its accessory structures. The four cars are the locomotive, passenger car 1, passenger car 2 and passenger car 3, respectively. The overall length is 101.29 m. The locomotive height is 4.736 m, and the passenger car's height is 4.433 m.

The computational domain is illustrated in Fig. 3. The height of the passenger car is chosen as a characteristic length and is denoted by h. The coordinate dimensions are denoted by x in the stream wise direction, y in the span-wise direction and z in the vertical direction. Given the full development of flow fields and the wake disturbance, the Inlet-1was located 36.1 h upstream of the head car and the crosswind entrance boundary, Inlet-2, was 36.1 h far from the center of the track. The height was 22.6 h. Then, the length, width and height of the computational zone were 112.8 h, 90.2 h and 22.6 h, respectively. The entire domain was treated as unstructured grids. As regards the numerical prediction, the grids that were near the surface of the train were refined. The surface mesh of a single passenger car is shown in Fig. 4. A standard wall function implemented in the Fluent software is adopted on the train surface when most of y+ is in the range of 30-300 in the paper. Before a decision on the mesh resolution used is made, three different meshes have been tried and the results can be found in Table 1. In addition, compared with the full-scale experimental data in Section 5.2, the medium mesh and the numerical method are suitable for computing the flow fields around trains.

For all numerical simulations the inlet condition was a uniform velocity profile that is constant in time. Velocities V_t and V_w are imposed, respectively. Where, V_t is the train speed and V_w is the crosswind speed. The upstream velocity $V_t = 0$, 40, 80, 120 and 160 km/h, and the crosswind speed $V_w = 41.4$, 50.9 and 60 m/s, separately. The surface of the train is set as no slip walls, and the ground, windbreak wall and track bed are moving walls. At the top of the computational domain, the symmetry is set. The outlet boundary condition was given by a static pressure of zero.
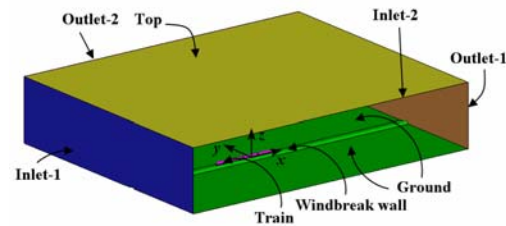
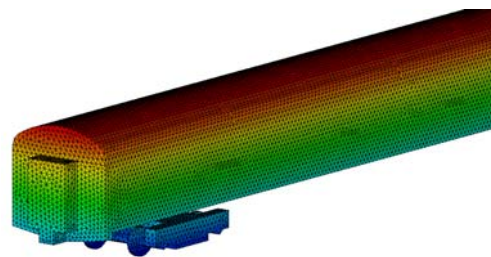

Fig. 3. Computational domain.

Fig. 4. Surface mesh of a single passenger car.

Table 1 Results for different mesh resolutions

Case	Number of Cells	C_s	C_l	C_M
Coarse mesh	2.6 millions	4.05	6.39	3.28
Medium mesh	4.5 millions	4.18	6.73	3.41
Fine mesh	6.5 millions	4.21	6.80	3.43

4. DESIGNED IDEAS AND PROJECTS

With the increment of the train speed and the electrification construction along the Lanzhou-Xinjiang railway, the windbreak effect of the original earth embankment type windbreak wall cannot meet the operational safety requirements, which has a great effect on the crosswind stability of speed-raising trains and the quality of the pantograph-catenary current collection for a locomotive. Therefore, urgent measures are required to conduct to optimize the aerodynamic shapes of windbreak walls.

To obtain the best shielding effect, economic practicality and feasibility must be also taken into account. Therefore, it is hard to reconstruct windbreak walls to a large extent. Zhang and Liu

(2014) discovered that the windward side (WWS) of a straight type windbreak wall (such as the reinforcement type, concrete plate type, and so on) is a vertical shape, which causes the flow over the top of the wall and obtains a raising angle, so the airflow can pass over the train. As a result, the train is in a favorable windbreak performance environment.

To optimize the aerodynamic shape of the earth embankment type, we can use the basic principle of the straight type for reference. Two designed projects will be discussed in the following sections. One is the heightening type whereby a length of straight wall is built on the top of the original type. The other is the cutting type that is cut out a step on its WWS. All these projects are shown in Fig. 5. The top of the original type is defined as the reference plane. In Fig. 4, H is separately chosen as 0.2, 0.3 and 0.4 m, and L is 1.0, 1.5 and 2.0 m, respectively.
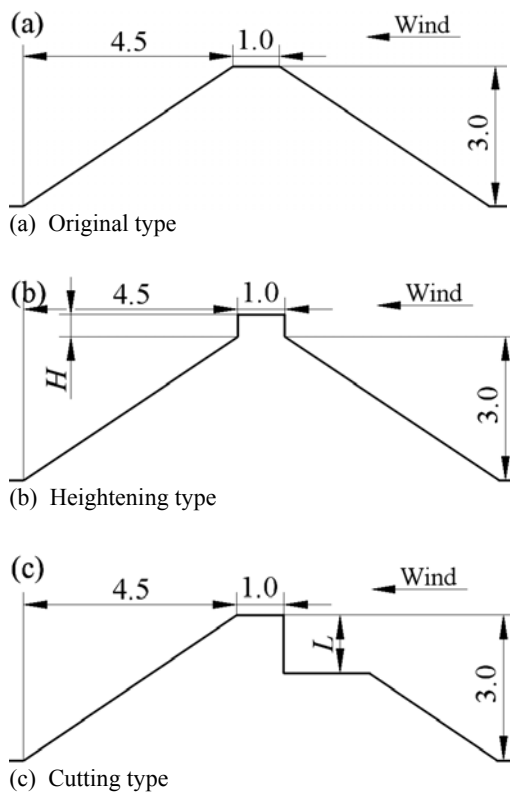

(a) Original type

(b) Heightening type

(c) Cutting type

Fig. 5. Cross-sections (unit: m).

5. RESULTS AND DISCUSSION

5.1 Data Processing

Aerodynamic forces include the side force, lift force and overturning moment are the significant factors to evaluate the aerodynamic performances of trains under cross winds. So the non-dimensional coefficients define as follows.

$$C_s = F_s/(qA), \ C_l = F_l/(qA), \ C_M = M/(qAh) \qquad (7)$$

Where, $q = 0.5\rho(V_t^2 + V_w^2)$, q is the dynamic pressure.

V_t is the speed of a train, while V_w is the wind speed. F_s, F_l and M are the side force, lift force and overturning moment respectively, corresponding to the C_s, C_l and C_M. A is the reference area which is 10 m² in analysis. h is the height of passenger cars. ρ is the constant air density that is 1.177 kg/m³ according to section 1.

At last, the non-dimensional coefficient of static pressure on the train body C_p also needs to define (Corin *et al.* 2008, Flynn *et al.* 2014, Osth and Krajnovic 2014).

$$C_p = (p - p_{ref})/q \qquad (8)$$

Where, p is the static pressure on train body. p_{ref} is the reference pressure.

5.2 Assessment of the Numerical Accuracy of the Simulation

Khier *et al.* (2000), Zhang *et al.* (2015), Zhang and Liu (2012, 2014), Tian (2015) and Liu *et al.* (2016) all suggest that the k-ε turbulence model in current paper can be used to compute the flow field around trains and windbreak walls. In addition, the experimental data in the report (Central South University 2011) are also used to validate the accuracy of the present numerical method. The experiments were based on the comprehensive full-scale tests of aerodynamic performances of trains and windbreak facilities along the Lanzhou-Xinjiang railway under strong winds. These tests were carried out from March 2009 to June 2009 by the Urumqi Railway Bureau. In the numerical simulation, the wind speed is equal to that in the test, 26.8 m/s, and the windbreak wall is the earth embankment type. The investigated vehicle is a single passenger car that is a 25 type with the same grouping model as in the test. Under strong wind conditions, the side force F_s, lift force F_l and overturning moment M are mainly influenced by the surface pressure of trains, and the air viscous effect is limited. Thus, based on the pressure of measure points, the Block Integral Method (Xiong *et al.* 2006) is used to calculate the aerodynamic forces. Table 2 shows the validation results in this program. It presents good agreement with the experimental and simulation results. The present numerical method is reasonable and could be used in further study.

Table 2 Comparison between the numerical simulation and the full-scale test

Method	C_s	C_l	C_M
Full-scale test	4.44	7.48	3.59
Numerical simulation	4.18	6.73	3.41
Error	5.9%	10.0%	5.0%

5.3 Aerodynamic Loads

To analyze and improve the crosswind stability of trains, the direct parameter is the aerodynamic load. According to publications (Tanemoto *et al.* 2006, Rezvani and Mohebbi 2014, Wang *et al.* 2014), the overturning moment, affected by the combination

with the side force and lift force, is an important criterion for the overturning of vehicles. Afterwards, the overturning moment coefficient C_M is investigated. A locomotive's weight is much heavier than that of a single passenger car, and the flow structures around the passenger car 1 and passenger car 3 are impacted by the air from the locomotive and in the wake, so the flow around the passenger car 2 is relatively equilibrium is chosen as the research vehicle. In section 5.3.1, trains are severally located on the windward line (WWL) and leeward line (LWL) at the stationary condition, and different crosswind speeds are set for studying the variations of overturning moment relative to the raising height and the cutting depth. Then, in section 5.3.2, the train is running at the speed of 40, 80, 120 and 160 km/h, and the crosswind speed is chosen as 41.4 m/s.

5.3.1 Stationary Condition

When the passenger train is in a stationary situation, the wind direction is chosen as 90° (it is perpendicular to the railway line.) with speeds of 41.4, 50.9 and 60.0 m/s, respectively. Fig. 6 shows the trend of the overturning moment coefficients as a function of the raising height, as the trains stand on the WWL and LWL.
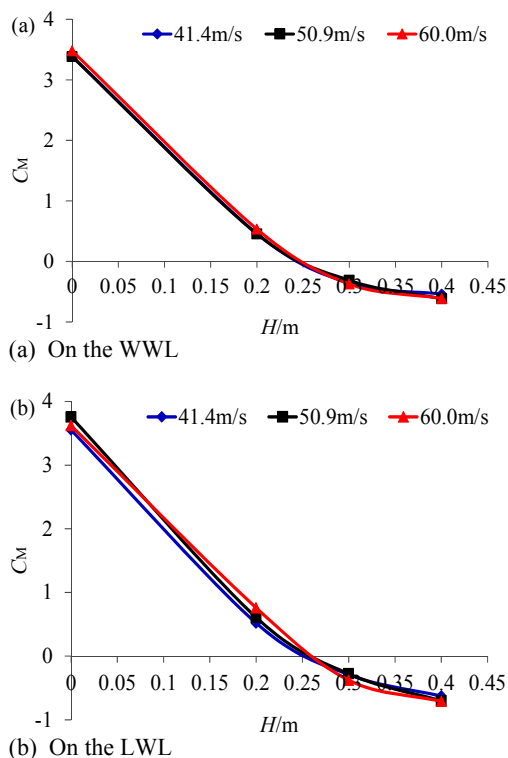
to be much less. When the height H varies from 0.24 m to 0.26 m, a height with the overturning moment of zero can be found. At this key point, the best windbreak performance is considered to be achieved. After that, the direction of the overturning moment reverses. When H=0.3 m, its growth rate slows down. Compared with the coefficients at the same height, it is discovered that they are not sensitive to the wind velocity. Meanwhile, when the car stand on the windward and leeward tracks at the crosswind behind the original windbreak walls, it presents that the LWC (leeward case) is more critical than the WWC (windward case) for the insufficient shielding effect of the walls. Thus, a higher straight wall is needed to build on the top of the earth embankment to insure the safety of trains on the leeward line. It can be deduced that the best height for the heightening type is about 0.26 m with the train in a stationary condition.

Figure 7 shows the interpolating curves of the overturning moment coefficients relative to the cutting depth with the train on the WWL or LWL. By means of the above same analysis method, the best depth with the overturning moment of zero is found, as the depth L is between 1.10 m and 1.20 m. Thus, it is concluded that the static optimal depth of the cutting type is about 1.20m.
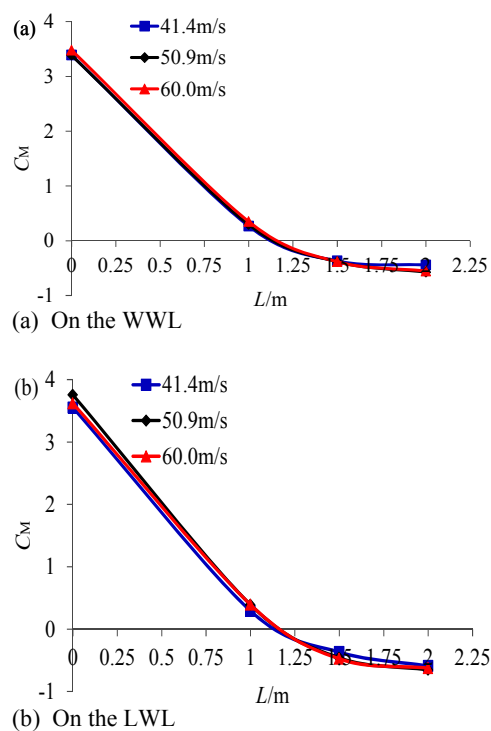

(a) On the WWL

(b) On the LWL

Fig. 6. Trend of the overturning moment coefficients as a function of the raising height at different wind speeds.

(a) On the WWL

(b) On the LWL

Fig. 7. Trend of the overturning moment coefficients as a function of the cutting depth at different wind speeds.

5.3.2 Running Condition

Behind the original type windbreak wall (that is H = 0 m), the car's moments are much larger than these behind these optimized projects, deviating from the windbreak wall, no matter on which line the car stands. As the height H increases, the moments tend

The above analysis shows that the optimal dimensions for the designed projects are not sensitive to the wind speed varying from 41.4 m/s to 60 m/s. In fact, the trains always run at different speeds under strong winds. In this section, the train

speed is chosen as 40, 80, 120 and 160 km/h, respectively, and the crosswind speed is 41.4 m/s. Fig. 8 and Fig. 9 show the trend of the overturning moment coefficients as a function of the raising height and cutting depth, when the trains with different speeds running on the WWL and LWL. At different train speeds, the variations of curves are basically the same. However, the lower the train speed is, the higher the C_M is. These results depend on the dynamic pressure and yaw angle. When the crosswind speed and direction is constant, the train speed is higher, the dynamic pressure is increased and the yaw angle is reduced. After that, the coefficient is less.
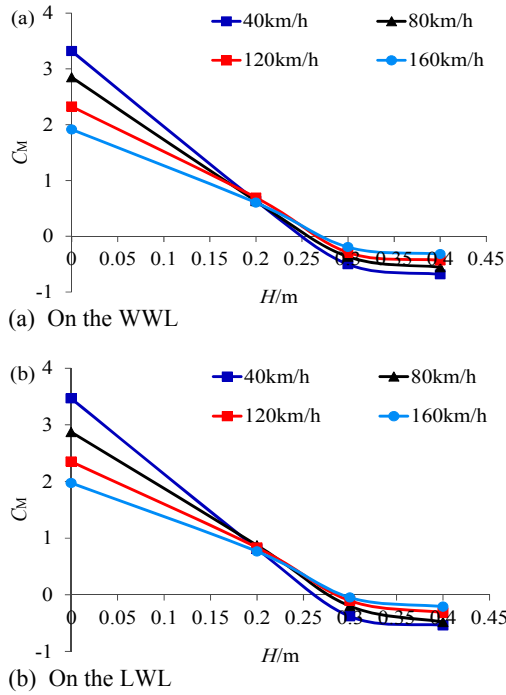

(a) On the WWL

(b) On the LWL

Fig. 8. Trend of the overturning moment coefficients as a function of the raising height at different train speeds.

According to the static analysis method in Section 5.3.1, the optimal sizes at different train speeds are obtained, as shown in Table 3.

The optimal sizes increase with increasing train speeds. When the train is stationary, the sizes are undoubtedly at the lowest. For the optimization projects, at the same speed, the size with the train on the WWL is slightly less.

After a comprehensive analysis and comparison of the calculation results at different wind and train speeds were performed, and given the train running safety requirements, the best height of the heightening type is about 0.30 m, and the optimal depth of the cutting type is 1.40 m.

5.4 Flow Field Structures Around the Train

The calculated flow fields in the cross-section at the middle of the passenger car 2 in the running direction of trains are depicted in the following figures in terms of static pressure.
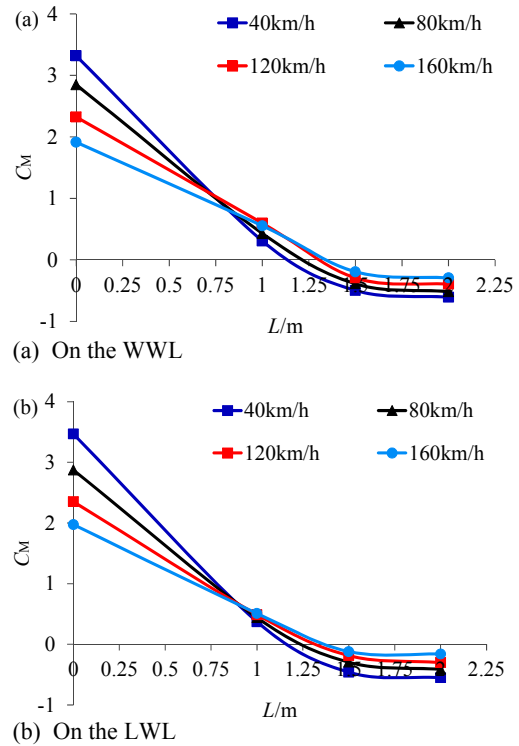

(a) On the WWL

(b) On the LWL

Fig. 9. Trend of the overturning moment coefficients as a function of the cutting depth at different train speeds.

Table 3 Optimal sizes of two projects at different train speeds

Project	V_t/(km/h)	Optimal size/m	
		WWL	LWL
Heightening type	0	0.240	0.255
	40	0.249	0.264
	80	0.260	0.276
	120	0.267	0.285
	160	0.272	0.290
Cutting type	0	1.10	1.12
	40	1.17	1.19
	80	1.27	1.29
	120	1.30	1.32
	160	1.35	1.37

When the train is stationary in a wind environment of 41.4 m/s, as illustrated in Fig. 10, behind the original type windbreak wall, the airflow could climb over the top of the windbreak wall, and then it directly acts on the train body. On the WWS of the train, a large area of positive pressure comes into being, and on its leeward side (LWS), there is a region with minor negative pressure. All these would lead to the train suffering a large lateral force. Above the train, the airflow rising over it accelerates considerably, which contributes to a strong negative pressure region to lower the running stability of the train further. Behind the optimization
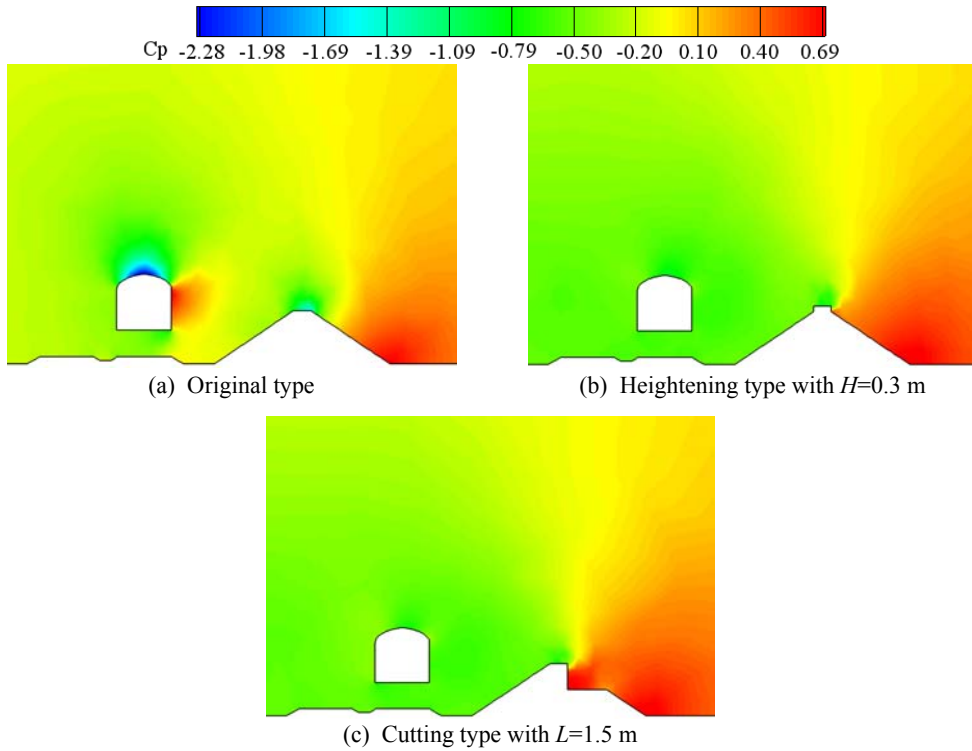
Cp -2.28 -1.98 -1.69 -1.39 -1.09 -0.79 -0.50 -0.20 0.10 0.40 0.69

(a) Original type

(b) Heightening type with *H*=0.3 m

(c) Cutting type with *L*=1.5 m

Fig. 10. Pressure distributions around the stationary trains.

Cp -1.38 -1.20 -1.02 -0.84 -0.66 -0.48 -0.30 -0.12 0.06 0.24 0.42

(a) Original type

(b) Heightening type with *H*=0.3 m

(c) Cutting type with *L*=1.5 m

Fig. 11. Pressure distributions around the running trains.

projects, due to the straight side on their WWSs, the wind cannot blow towards the train directly so the whole train is basically in a negative pressure environment. However, a minor negative pressure focuses on the top. When the train runs at a speed of 120 km/h with a crosswind speed of 41.4 m/s, as shown in Fig. 11, behind the original type windbreak wall, there is a slight difference between the train with and without speed. The area of positive pressure on the WWS of the train and the

region of negative pressure on the top are both reduced. Behind the optimization projects, it seems that the train speed has a limited effect on the pressure distributions. The train is in a favorable windbreak performance environment, and a relatively balanced pressure environment around the train is formed.

5.5 Surface Pressure Coefficient Distributions

When the trains stand on the tracks subjected to a crosswind at the velocity of 41.4 m/s, the surface pressure coefficient distributions are illustrated in Fig. 12(a). Correspondingly, when the trains with the train speed of 120 km/h stand on the tracks subjected to a crosswind at the velocity of 41.4 m/s, the surface pressure coefficient distributions are illustrated in Fig. 12(b). The cross-section is set in the middle plane of the passenger car 2 along the running direction of the train. P_e is the earth embankment type. P_h is the heightening type with H=0.3 m and P_c is the cutting type with L=1.5 m.

When the train is stationary, behind the original type windbreak wall, the positive C_p takes up the dominant role on the WWS of the train. The top, LWS and bottom are all with negative pressure. The maximum of C_p is 0.74 while the train stands on the WWL, and its corresponding minimum is -2.36. The peak-to-peak value is 3.10, so the passenger car is in a very serious pressure environment. Along the curve of the cross-section, at the transition, such as points *b*, *c* and *e*, due to geometry structure with the arc-shape and corner, C_p takes place a rapid change, while it is smoother at point *f*. Behind the optimization projects, C_p on the train surface is negative. For the heightening type, when the train is on the WWL, the maximum of C_p is -0.40, and its minimum is -0.91. The peak-to-peak value is 0.51 and it is larger than that of the train on the LWL with a value of 0.38. For the cutting type, as the train stands on the WWL, the maximum of C_p is -0.30, and its minimum is -0.78. The peak-to-peak value is 0.48 and it is less than that of the train on the LWL with the value of 0.53. Thus, these peak-to-peak values indicate that the optimization projects could enhance the windbreak effect at least five times more than the original type.

When the train runs at a certain speed, behind the original type windbreak wall the variation of the curve is similar to that without the train speed. However, for the limited shield effect of the original earth type, when the train is on the WWL, the maximum of C_p is 0.32, and its minimum is -1.28. The peak-to-peak value is 1.60 and it is almost half that of the one without train speeds. For the heightening type, as the train is running on the WWL, the maximum of C_p is -0.24, and its minimum is -0.79. The peak-to-peak value is 0.54 and it is larger than that of the train on the LWL with the value of 0.52. For the cutting type, when the train is running on the WWL, the maximum of C_p is -0.15, and its minimum is -0.75. The peak-to-peak value is 0.60 and it is also larger than that of the train on the LWL with the value of 0.50.

Therefore, according to these peak-to-peak values, the optimization projects would enhance the windbreak effect more than three times as much as the original type. Regardless of the train is at the stationary or running condition, all the evidence shows that the optimization projects can be put into practice.
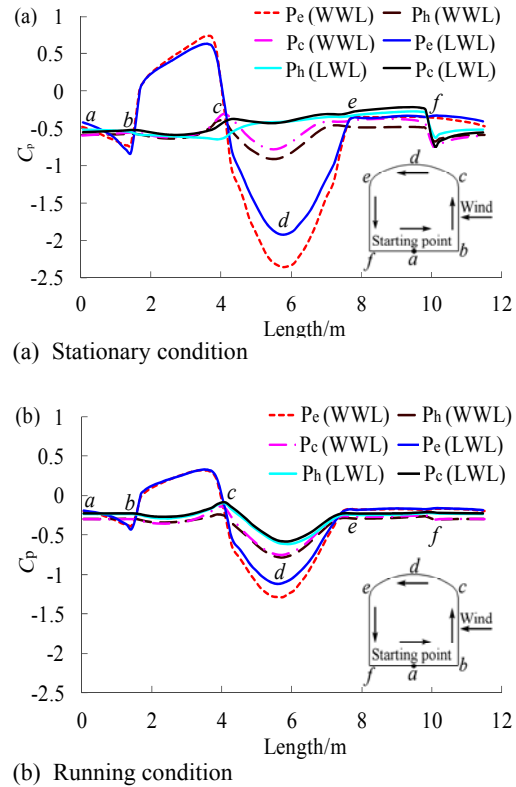

(a) Stationary condition

(b) Running condition

Fig. 12. Surface pressure coefficient distributions.

5.6 Lateral wind speed at the catenary position

Wind speed is an important factor in the catenary design, and it is also the basic principle for governing calculations. It affects not only the stability of the main chondrophone of a catenary, but also the quality of the pantograph-catenary current collection for the locomotive. Thus, the lateral wind speed at the catenary position which is the lateral component of the resultant speed coming from the train speed and crosswind speed has an important effect on system security. The electrification of the Lanzhou-Xinjiang railway line has now been completed. It is very important to study the lateral wind speed at the catenary position under the original type windbreak wall and optimization projects to improve the quality of the pantograph-catenary current collection. The curves of lateral wind speeds with a function of the height/depth of the wall added/cut are demonstrated in Fig. 13. When there is no train on the lines, the incoming crosswind speed is 41.4 m/s. Otherwise, the wind speed is a constant of 41.4 m/s, and the train is running at a speed of 120 km/h.
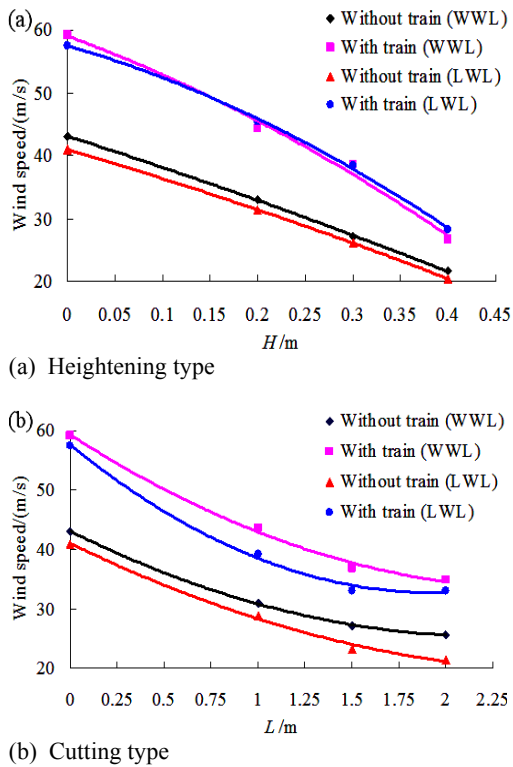
(a) Heightening type

(b) Cutting type

Fig. 13. Curves of lateral wind speeds.

Behind the original type windbreak wall (that is, H=0 m or L=0 m), without trains on railway lines, the lateral wind speed above the LWL at the catenary position is less than that of the WWL. As the train runs on the windward or leeward lines, the corresponding lateral wind speed rise sharply by 37.5% and 40.5%, respectively.

After adoption of the heightening type, without trains on railway lines, the speeds of the two lines monotonically decrease. When H=0.3 m, compared with the wind speed behind the original type, the lateral wind speeds is reduced by 37.0% and 36.1% on the WWL and LWL, respectively. When the train passes through the railway line, the wind speeds are decreased with the increment of height. As H=0.3 m, the lateral wind speeds on the WWL and LWL separately are reduced by 34.7% and 33.2%.

Behind the cutting type, when L=1.5m, without trains on the railway lines, compared with the wind speed behind the original type, the lateral wind speeds on the WWL and LWL are reduced by 37.0% and 43.1%, respectively. As the train passes through the railway line, the lateral wind speeds on the WWL and LWL separately are reduced by 37.7% and 42.5%. According to the comprehensive comparison, the effect of the height type on reducing wind speed is better.

6. CONCLUSIONS

An obstacle will result in a shielding effect on the bodies behind it. Based on this, hundreds of kilometers windbreak walls have been built along

the Lanzhou-Xinjiang railway line. The aerodynamic performances of trains are much better than the one without windbreak walls. However, if the height of the windbreak wall with an inclined windward side is lower than the train's top, like the earth embankment type windbreak wall, the shielding effect will be not enough. The airflow still can act on the train body. After that, as the train is running at a higher speed, it is still in a danger. In addition, according to the full-scale aerodynamic experiments conducted from March 2009 to June 2009 along the Lanzhou-Xinjiang railway under strong winds, it indicates that one of the worst locations in terms of train aerodynamic characteristics and dynamic performances is the district with the earth embankment type windbreak wall. Thus, to promote the windbreak effect of the earth embankment type windbreak wall, enhance the operational speed of the single passenger train and improve the quality of the pantograph-catenary current collection for a locomotive, two designed projects were discussed in the paper. One was the heightening type whereby a length of straight wall is built on the top of the original type. The other was the cutting type that is cut out a step on its WWS.

Validation was performed against full-scale experimental data, which presents reasonable agreement accordance with the experimental and simulation results. The relationships between the overturning moment of the train, the lateral wind speed at the catenary position and the height (depth) in optimization projects were analyzed. In addition, to understand the flow field around the train with different types of windbreak walls, pressure contours and surface pressure coefficient distributions were investigated. Based on the results and discuss, the study shows that:

(1) Behind the original earth embankment type windbreak wall, the flow can directly act on the train body, and the overturning moment coefficient of the passenger car is much larger, no matter on which line the car is running. However, behind the optimization projects, as the height/depth increases, the overturning moment coefficient becomes much less. These cars are basically in a minor negative pressure environment.

(2) The optimal heights for the heightening type/depths for the cutting type do not change obviously as the train speed increases. When the passenger car is stationary, the optimal height/depth is the smallest.

(3) Behind the original type, the lateral wind speed at the catenary position above the leeward line is less than that of the windward line. When the train passes through the WWL or LWL, the speeds rise sharply. After adoption of the optimized projects, the speeds of the two lines monotonically decrease. The effect of the height type on reducing wind speed is better.

(4) The best height of the heightening type is 0.30 m, and the optimal depth of the cutting type is 1.40 m.

In conclusion, the two designed projects can improve the windbreak performance, while the heightening type contributes to the engineering application.

REFERENCES

Asgharzadeh, H., B, Firoozabadi and H. Afshin (2012). Experimental and Numerical Simulation of the Effect of Particles on Flow Structures in Secondary Sedimentation Tanks. *Journal of Applied Fluid Mechanics*, 5(2), 15-23.

Baker, C. J. (1986). Train Aerodynamic Forces from Moving Model Experiments. J*ournal of Wind Engineering and Industrial Aerodynamics* 24(3), 227-252

Baker, C. J. (2010). The flow around high speed trains. *Journal of Wind Engineering and Industrial Aerodynamics* 98(6), 277-298.

Baker, C. J. (1999). The wind tunnel determination of crosswind forces and moments on a High Speed Train. *Proceedings of the TRANSAERO Symposium*, May 04-05, 1999.

Bocciolone, M, F. Cheli, R. Corradi, S. Muggiasca and G. Tomasini (2008). Crosswind action on rail vehicles: Wind tunnel experimental analyses. *Journal of Wind Engineering and Industrial Aerodynamics* 96, 584-610.

Central, South University (2011). Research report for train aerodynamic performance tests. *Changsha: Central South University.* (in Chinese)

Cheli, F., F. Ripamonti, D. Rocchi and G. Tomasini (2010). Aerodynamic behaviour investigation of the new EMUV250 train to cross wind. *Journal of Wind Engineering and Industrial Aerodynamics* 98, 189-201.

Corin, R. J., L. He and R. G. Dominy (2008). A CFD investigation into the transient aerodynamic forces on overtaking road vehicle models. *Journal of Wind Engineering and Industrial Aerodynamics*, 96, 1390-1411.

Diedrichs, B., M. Sima, A. Orellano and H. Tengstrand (2007). Crosswind stability of a high-speed train on a high embankment. *Proceedings of the Institution of Mechanical Engineers, Part F: Journal of Rail and Rapid Transit* 221(2), 205−225.

Fauchier, C., E. Devehat Le and R. Gregoire (1999). Numerical study of the turbulent flow around the reduced-scale model of an Inter-Regio. *Proceedings of the TRANSAERO Symposium*, Paris, France, May 04-05, 1999.

Fluent Inc. *FLUENT User's Guide,* 2006.

Flynn, D., H. Hemida, D. Soper and C. Baker (2014). Detached-eddy simulation of the slipstream of an operational freight train. *Journal of Wind Engineering and Industrial Aerodynamics*, 132, 1-12.

Fujii, T., T. Maeda, H. Ishida, T. Imai, K. Tanemoto and M. Suzuki (1999). Wind-Induced Accidents of Train/Vehicles and Their Measures in Japan. *Quarterly Report of Railway Technical Research Institute* 40(1), 50-55.

Ge, S. C. and F. Q. Jiang (2009). Analyses of the Causes for Wind Disaster in Strong Wind Area along Lanzhou-Xinjiang Railway and the Effect of Windbreak. *Journal of railway engineering society* 5, 1-4. (in Chinese)

Hemida, H. and S. Krajnovic (2010). LES study of the influence of the nose shape and yaw angles on flow structures around trains. *Journal of Wind Engineering and Industrial Aerodynamics* 98, 34−46.

Khier, W., M. Breuer and F. Durst (2000). Flow structure around trains under side wind conditions: a numerical study. *Computer&Fluids* 29, 179-195.

Liu, F. H. (2006). Wind-proof effect of different kinds of wind2break walls on the security of trains. *Journal of Central South University: Science and Technology* 37(1), 176-182.

Liu, T. H., X. C. Su, J. Zhang, Z. W. Chen and X. S. Zhou (2016). Aerodynamic performance analysis of trains on slope topography under crosswinds. *Journal of Central South University* 23(9), 2419-2428.

Liu, T. H. and J. Zhang (2013). Effect of landform on aerodynamic performance of high-speed trains in cutting under cross wind. *Journal of Central South University* 20(3), 830-836.

Munoz Paniagua, J., J. García, A. Crespo and F. Laspougeas (2015). Aerodynamic Optimization of the Nose Shape of a Train Using the Adjoint Method. *Journal of Applied Fluid Mechanics* 8(3). 601-612.

Osth, J. and S. Krajnovic (2014). A study of the aerodynamics of a generic container freight wagon using Large-Eddy Simulation. *Journal of Fluids and Structures* 44, 31-51.

Rezvani, M. A. and M. Mohebbi (2014). Numerical calculations of aerodynamic performance for ATM train at crosswind conditions. *Wind and*

Structures 18(5), 529-548.

Tanemoto, K., M. Suzuki and H. Fuji (2006). Wind tunnel experiments on aerodynamic characteristics of vehicle crosswind. *Railway Research Review* 63(8), 28-31.

Tian, H. Q. (2007). Train aerodynamics. *Beijing: China Railway Housing Press* 30-32.

Tian, H. Q. (2015). Determination method of load balance ranges for train operation safety under strong wind. *Journal of Central South University* 22(3), 1146-1154.

Tomasini, G., S. Giappino, F. Cheli and P. Schito (2016). Windbreaks for railway lines: Wind tunnel experimental tests. *Proceedings of the Institution of Mechanical Engineers, Part F: Journal of Rail and Rapid Transit* 230(4), 1270-1282.

Wang, B. S. (2010). Analysis and Optimization of Aerodynamic Performance of Train at Transitional Zone Between Cut and Wind-Break Walls. *2010 International Conference on Optoelectronics and Image Processing: IEEE*, Haiko, China 11, 234-238.

Wang, H. X., S. D. Wang, Z. Gao and B. Y. Zhang (1990). The effects of wind break engineering on wind characteristics and lateral aerodynamic characteristics of railway cars. *Acta Aerodynamica Sinica* 8(4), 430-436.

Wang, Y., Y. Xin, Z. Gu, S. Wang, Y. Deng and X. Yang (2014). Numerical and Experimental Investigations on the Aerodynamic Characteristic of Three Typical Passenger Vehicles. *Journal of Applied Fluid Mechanics* 7(4), 659-671.

Xiong, X. H., X. F. Liang, G. J. Gao and T. H. Liu (2006). Train aerodynamic characteristics in strong cross2wind on Lanzhou2Xinjiang railway line. *Journal of Central South University: Science and Technology* 37(6), 1183-1188.

Zhang, J., G. J. Gao, T. H. Liu and Z. W. Li (2015). Crosswind stability of high-speed trains in special cuts. *Journal of Central South University* 22(7), 2849-2856.

Zhang, J. and T. H. Liu (2012). Optimization Research on the Slope Angle of the Earth Type Windbreak Wall of Xinjiang Single-Track Railway. *China Railway Science* 33(2), 28-32.

Zhang, J. and T. H. Liu (2014). Multistep design of earth type windbreak wall along Lanzhou-Xinjiang railway. *Journal of Central South University: Science and Technology* 45(4), 1334-1340.